

Optical Absorption Spectra of Aromatic Isothianaphthene Oligomers: Theory and Experiment

C. Quattrocchi, R. Lazzaroni,[†] and J. L. Brédas*

Service de Chimie des Matériaux Nouveaux, Centre de Recherche en Electronique et Photonique Moléculaires, Université de Mons-Hainaut, Place du Parc 20, B-7000 Mons, Belgium

R. Kiebooms, D. Vanderzande, and J. Gelan

Instituut voor Materiaalonderzoek (IMO), Divisie Scheikunde, Universitaire Campus, Limburg University, B-3590 Diepenbeek, Belgium

L. Van Meervelt[‡]

Laboratorium voor Macromoleculaire Structuurchemie, Katholieke Universiteit of Leuven, Celestijnenlaan 200F, B-3001 Leuven, Belgium

Received: June 17, 1994; In Final Form: September 21, 1994[®]

We investigate the optical absorption spectra of aromatic isothianaphthene oligomers, from the monomer up to the tetramer, with a combined theoretical and experimental approach. Geometry optimizations are performed with the semiempirical Austin Model 1 method on disilylated isothianaphthene oligomers of increasing chain length. The calculated geometric parameters are compared to those obtained from the single-crystal structure of the 3,3'-bis(*tert*-butyldimethylsilyl)-1,1'-biisothianaphthene. We then use the intermediate neglect of differential overlap method, coupled to single configuration interaction, to simulate theoretically the optical absorption spectra of the oligomers. The corresponding experimental spectra are recorded in *n*-hexane solution, and their evolution with chain length is discussed on the basis of the theoretical data.

1. Introduction

Conjugated polymers are at present intensively studied because of their increasing technological potential applications.¹ Much attention has been devoted to the synthesis of low-band-gap polymers, *i.e.*, macromolecular materials which could be intrinsically good electrical conductors without the need of doping. Polyisothianaphthene (PITN) is prototypical for this class of polymers; it presents an experimental band gap of 1 eV.² Over the past few years, theoretical and experimental efforts have been devoted to the determination of the ground-state geometry of the polymer,^{3–8} which had been the object of controversy in the literature. Recently, we have been in a position to confirm by means of a joint experimental and theoretical study that the quinoid form is slightly more stable than its aromatic counterpart.^{7,8} However, since the two forms are almost isoenergetic, both structures could actually exist, depending, for instance, on the polymerization route.

According to quantum-chemical modeling,^{3,5,7} the nature of the end groups and the geometric structure of the chains are directly related; it has been shown that systems where the terminal α carbons are linked by a single bond to the external group (Figure 1a) present an aromatic character. This result is confirmed by the work of Okuda *et al.*⁹ who have prepared *tert*-butyldimethylsilyl-substituted oligomers which possess an aromatic structure. The quinoid structure is obtained by either adding a second hydrogen atom or attaching a double bond to each of the terminal α carbon sites (Figure 1b).

The band structure of PITN has been calculated^{7,10} by means of the valence effective Hamiltonian (VEH) method;¹¹ the results indicate that the aromatic polymer should possess a band-gap

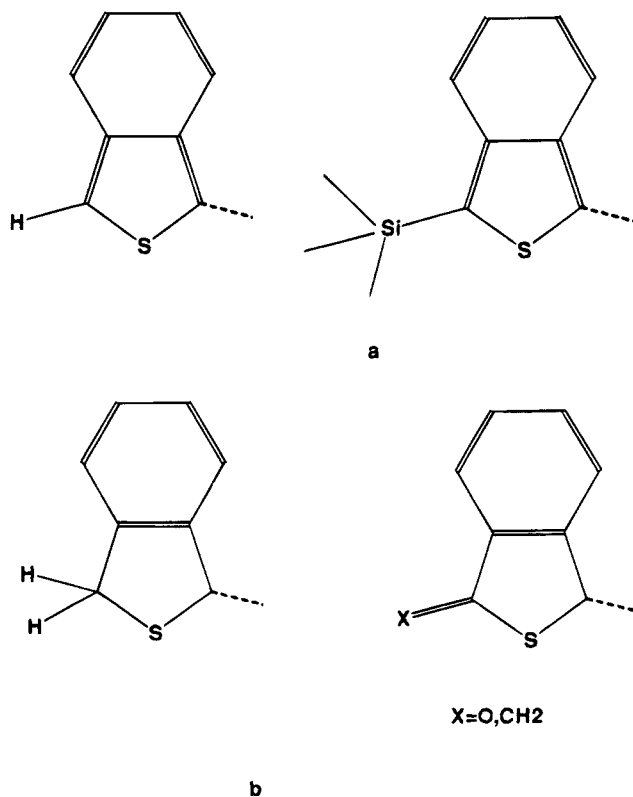


Figure 1. Illustration of the different chain ends in isothianaphthene oligomers. The molecules extend to the right-hand side of the structures.

even smaller than that of quinoid PITN (0.2–0.6 vs 1.2 eV). On the basis of this interesting feature, we have undertaken a theoretical and experimental study of the electronic properties

[†] Senior Research Associate of the National Fund for Scientific Research (Belgium).

[®] Abstract published in *Advance ACS Abstracts*, February 15, 1995.

of isothianaphthene oligomers (from the monomer up to the tetramer) capped by disilylated groups. The investigation of aromatic oligomers of increasing size should lead to improved understanding of the electronic properties, in particular the optical absorption spectrum, of aromatic PITN chains.

As a first step, geometry optimizations are carried out on a series of isothianaphthene oligomers at the semiempirical Austin Model 1 (AM1) level.¹² This method is parameterized to give good estimates of geometries and heats of formation of organic compounds. The theoretical data are compared to the results of X-ray diffraction experiments performed on a disilyl-substituted isothianaphthene dimer. (Attempts to grow large single crystals of longer oligomers have not been successful so far.) Based on the AM1-optimized geometries, the intermediate neglect of differential overlap (INDO) method,¹³ coupled to single configuration interaction (SCI),¹⁴ is then used to calculate the electronic transition energies and related oscillator strengths. In parallel, we have synthesized bis(*tert*-butyldimethylsilyl)-isothianaphthene oligomers from the monomer up to the tetramer, according to the method described by Okuda *et al.*⁹ The experimental optical absorption spectra, taken in *n*-hexane, are compared to the theoretical curves. The origin and the evolution of the experimental absorption peaks are analyzed on the basis of the calculated data.

2. Theoretical Methodology

Full geometry optimizations on bis(trimethylsilyl)isothianaphthene monomer and dimer and isothianaphthene trimer, tetramer, and hexamer are performed at the AM1 level with the MOPAC 6.0 package running on an IBM RISC/6000 workstation.

The INDO/SCI calculations are carried out using the ZINDO package developed by Zerner.¹⁵ The electronic configurations we consider are generated by promoting one electron from one of the 15 highest occupied molecular orbitals (HOMO) to one of the 15 lowest unoccupied levels (LUMO). The introduction of further levels, which we have done in order to test the validity of our approach, does not change the results in any significant way. The electron-electron repulsion terms are described *via* the Mataga-Nishimoto potential,¹⁶ which is the most appropriate to reproduce absorption spectra within the INDO/SCI formalism. The theoretical absorption spectra are simulated by means of a convolution with Gaussians whose full width at half-maximum is set at 0.2 eV.

We note that the geometries of the trimer, tetramer, and hexamer have been optimized without the silyl groups, due to the large size of the systems. This approximation is justified by the fact that the explicit consideration of the silyl groups in the dimer does not influence the lower-energy transitions in the optical absorption spectra.

3. Experimental Section

(a) Synthesis. The isothianaphthene oligomers were synthesized according to the method described by Okuda *et al.*⁹ However, the starting product, thiophthalic anhydride, was prepared according to the method of Reissert *et al.*¹⁷ THF was distilled on sodium/benzophenone, acetonitrile was distilled on CaH₂, and dichloromethane was distilled on phosphorus pentoxide. All compounds were crystallized prior to use. Phthalic anhydride was purchased from Janssen Chimica. Slow evaporation of a *n*-hexane/acetonitrile two-phase system gave the crystals of the dimer used in the single-crystal structure determination.

The ¹H and ¹³C NMR spectra of the compounds were obtained with a Varian Unity 400 spectrometer. All the spectra

were recorded in CDCl₃ (the chemical shifts of the carbon and the hydrogen being 77.0 and 7.24 ppm, respectively, from tetramethylsilane, TMS) at 30 °C. Assignments¹⁸ were based on the coupling patterns, the integration, the one-dimensional nuclear Overhauser effect (NOE), the attached proton tests (APT), and the two-dimensional ¹H-¹³C heteronuclear correlation (HETCOR) experiments optimized for $J_{CH} = 140$ Hz and $J_{CH} = 8$ Hz. The IR spectra were recorded with a Philips Pye Unicam SP-300. The FT-IR and the FT-RAMAN data were obtained *via* an IFS 66 FT-IR spectrometer (excitation wavelength: 1064 nm) connected with a Bruker computer (ASPECT 1000) accompanied with a Raman FRA 106 module. The mass spectra were obtained *via* a Finigan 1020 and a TSQ 70 apparatus. The UV-VIS spectra were recorded on a Perkin-Elmer Lambda 5 (transmission mode) using uvasol quality *n*-hexane (Merck). The concentrations of the oligomers were kept in the 1×10^{-4} to 1×10^{-5} M range, in order to maintain absorbance in the UV-vis region to reasonable levels.

Thiophthalic Anhydride.¹⁷ Forty grams (0.27 mol) of phthalic anhydride is thoroughly mixed with 80 g (0.33 mol) of sodium sulfide nonahydrate. The resulting liquid is stirred for 5 h. Addition of 100 mL of water gives a yellow solution which is added slowly to 2 L of HCl (5%). When the addition is completed, the mixture is stirred for an additional hour and filtered. The residue is dissolved in chloroform, washed with sodium hydrogenocarbonate (1 M) and water, and dried on magnesium sulfate. After crystallization from chloroform/*n*-hexane, 35 g of white thiophthalic anhydride crystals is obtained (yield 78%): mp 105.5 °C; FT-IR (KBr, ν , cm⁻¹) 1780, 1690, 1655, 1580, 1474, 1454, 1327, 1223, 949, 833, 783, 710, 455; MS (EI, *m/e*) 164 (M⁺), 104 (M⁺ - COS), 76 (M⁺ - (CO)₂S); ¹H NMR (CDCl₃, 400 MHz, relative to TMS) 7.82 (dd, 2, $J = 2.9, 5.1$ Hz), 7.97 (dd, 2, $J = 2.9, 5.1$ Hz); ¹³C NMR (CDCl₃, 400 MHz, relative to TMS) 123.7 (CH), 135.0 (CH), 138.7 (C), 189.8 (CO).

1,1,3,3-Tetrachlorothiophthalan.⁹ An intimate mixture of 24.6 g (0.15 mol) of thiophthalic anhydride and 78.0 g (0.37 mol) of phosphorus pentachloride is heated in an oil bath (150 °C) for 15 h. Phosphorus oxychloride formed during the reaction is evaporated under reduced pressure. Toluene (10 mL) is added and removed under reduced pressure (2x). The residue is dissolved in chloroform and washed with sodium hydrogen carbonate (1 M) and water. The organic phase is dried on magnesium sulfate and crystallized from *n*-hexane to yield 36.7 g of white crystals (90%): mp 111.5 °C; FT-IR (KBr, ν , cm⁻¹) 2773, 2692, 2631, 1975, 1933, 1813, 1710, 1635, 1474, 1454, 1231, 1180, 1099, 887, 806, 700, 610, 440; MS (EI, *m/e*) 237 (M⁺ - Cl), 202 (M⁺ - 2Cl), 167 (M⁺ - 3Cl); ¹H NMR (CDCl₃, 400 MHz, relative to TMS) 7.63 (dd, 2, $J = 3.1, 6.0$ Hz), 7.78 (dd, 2, $J = 3.1, 6.0$ Hz); ¹³C NMR (CDCl₃, 400 MHz, relative to TMS) 123.8 (CH), 131.5 (CH), 142.0 (C), 92.6 (CCl₂).

1,3-Bis(*tert*-butyldimethylsilyl)isothianaphthene.⁹ *n*-Butyllithium (0.14 mol, 9 g, 87.5 mL/1.6 M solution in *n*-hexane) is added dropwise to a stirred solution of 11 g (0.04 mol) of 1,1,3,3-tetrachlorothiophthalan in 160 mL of THF at -78 °C, followed by the addition of 15.1 g (0.1 mol) of *tert*-butyldimethylsilyl chloride in 30 mL of THF. The mixture is allowed to warm to room temperature and stirred for an additional 30 min. It is then poured in ice-water, extracted into *n*-hexane, and dried on magnesium sulfate. The obtained product is purified by column chromatography (silica, *n*-hexane) to give 13.7 g of a yellow crystalline solid (95%). Further purification by crystallization from chloroform/acetonitrile gives white crystals (yield 71%): mp 78 °C; FT-IR (KBr, ν , cm⁻¹) 3090,

2951, 2928, 2854, 2708, 1470, 1358, 1254, 1138, 1003, 964, 806, 768; FT-Raman (cm^{-1}) 3074 (m), 2957 (s), 2928 (s), 2900 (s), 2858 (s), 1512 (m), 1463 (m), 1448 (s), 1369 (s), 1358 (m), 1300 (m), 1200 (w), 1015 (m), 940 (w), 830 (w), 582 (m), 476 (m), 185 (w); MS (EI, *m/e*) 362 (M^+), 305 ($\text{M}^+ - \text{tert-butyl}$), 249, 233, 173, 159, 145, 131, 73, 57; ^1H NMR (CDCl_3 , 400 MHz, relative to TMS) 0.54 (s, 12, $\text{CH}_3\text{-Si}$), 0.98 (s, 18, $\text{CH}_3\text{-C}$), 7.11 (dd, 2, $J = 2.9, 6.7$ Hz, H_5), 7.83 (dd, 2, $J = 2.9, 6.7$ Hz, H_4); ^{13}C NMR (CDCl_3 , 400 MHz, relative to TMS) -3.9 (Si-CH_3), 18.2 ($\text{CH}_3\text{-C}$), 26.8 (C-CH_3), 135.0 (C_3), 146.5 (C_{3a}), 122.6 (C_5), 124.0 (C_4).

Oligomerization.⁹ A solution of 6.1 mL (55.1 mmol) of titanium tetrachloride in 60 mL of dichloromethane is added all at once at room temperature to a solution of 10 g (27.6 mmol) of 1,3-bis(*tert*-butyldimethylsilyl)isothianaphthene in 60 mL of dichloromethane. After being stirred for 10 h, the violet reaction mixture is poured into ice-water, extracted with ether, and dried on magnesium sulfate. The residue from ether is subjected to column chromatography (silica, *n*-hexane) to give the dimer (0.55 g), the trimer (0.34 g), and the tetramer (0.24 g). The resulting solids are further purified by crystallization from chloroform/acetonitrile.

Dimer: mp 145–147 °C; FT-IR (KBr, ν , cm^{-1}) 3059, 2951, 2928, 2854, 1466, 1389, 1358, 1250, 1007, 976, 806, 744; FT-Raman (cm^{-1}) 3074 (w), 2957 (w), 2928 (w), 2900 (w), 2858 (w), 1517 (w), 1497 (s), 1449 (s), 1428 (w), 1372 (w), 1320 (m), 1185 (w), 889 (vw), 755 (w), 578 (w), 475 (m), 199 (w); MS (EI, *m/e*) 494 (M^+), 437 ($\text{M}^+ - \text{tert-butyl}$); ^1H NMR (CDCl_3 , 400 MHz, relative to TMS) 0.56 (s, 12, $\text{CH}_3\text{-Si}$), 1.02 (s, 18, $\text{CH}_3\text{-C}$), 7.10–7.18 (m, 4, H_5 and H_6), 7.76 (m, 2, H_4), 7.86 (m, 2, H_7); ^{13}C NMR (CDCl_3 , 400 MHz, relative to TMS) -3.9 (Si-CH_3), 18.2 ($\text{CH}_3\text{-C}$), 26.8 (C-CH_3), 129.2 (C_3), 145.6 (C_{3a}), 123.9 (C_4), 123.7 (C_5), 123.6 (C_6), 122.0 (C_7), 137.5 (C_{7a}), 132.2 (C_1).

Trimer: FT-IR (KBr, ν , cm^{-1}) 3063, 2951, 2924, 2854, 1466, 1385, 1358, 1254, 1092, 1003, 980, 806, 768; FT-Raman (cm^{-1}) 3074 (vw), 2957 (vw), 2928 (vw), 2900 (vw), 2858 (vw), 1610 (vw), 1521 (vw), 1489 (m), 1448 (s), 1360 (w), 1331 (m), 1192 (w), 474 (w), 188 (w); MS (EI, *m/e*) 626 (M^+), 569 ($\text{M}^+ - \text{tert-butyl}$); ^1H NMR (CDCl_3 , 400 MHz, relative to TMS) 0.55 (s, 12, $\text{CH}_3\text{-Si}$), 1.02 (s, 18, $\text{CH}_3\text{-C}$), 7.14–7.18 (m, 6, $\text{H}_5[\text{A,B}]$ and $\text{H}_6[\text{A}]$), 7.75 (m, 2, $\text{H}_4[\text{A}]$), 7.86 (dd, 2, $J = 3.0, 7.0$ Hz, $\text{H}_4[\text{B}]$), 7.94 (m, 2, $\text{H}_7[\text{B}]$); ^{13}C NMR (CDCl_3 , 400 MHz, relative to TMS) -3.9 (Si-CH_3), 18.2 ($\text{CH}_3\text{-C}$), 26.8 (C-CH_3), 129.8 ($\text{C}_3[\text{A}]$), 145.6 ($\text{C}_{3a}[\text{A}]$), 124.0 ($\text{C}_4[\text{A}]$), 123.8 ($\text{C}_5[\text{A}]$), 123.9 ($\text{C}_6[\text{A}]$), 121.9 ($\text{C}_7[\text{A}]$), 137.6 ($\text{C}_{7a}[\text{A}]$), 131.6 ($\text{C}_1[\text{A}]$), 126.7 ($\text{C}_3[\text{B}]$), 136.5 ($\text{C}_{3a}[\text{B}]$), 121.9 ($\text{C}_4[\text{B}]$), 124.7 ($\text{C}_5[\text{B}]$).

Tetramer: FT-IR (KBr, ν , cm^{-1}) 3063, 2951, 2924, 2854, 1466, 1408, 1358, 1254, 1007, 976, 806, 768; FT-Raman (cm^{-1}) 1641 (w), 1486 (w), 1444 (s), 1355 (w), 1333 (s), 1196 (w), 1151 (w), 977 (w), 892 (w), 749 (w), 470 (w), 185 (w); MS (EI, *m/e*) 758 (M^+), 701 ($\text{M}^+ - \text{tert-butyl}$); ^1H NMR (CDCl_3 , 400 MHz, relative to TMS) 0.55 (s, 12, $\text{CH}_3\text{-Si}$), 1.02 (s, 18, $\text{CH}_3\text{-C}$), 7.12–7.20 (m, 8, $\text{H}_5[\text{A,B}]$ and $\text{H}_6[\text{A,B}]$), 7.76 (m, 2, $\text{H}_4[\text{A}]$), 7.89 (m, 2, $\text{H}_4[\text{B}]$), 7.99 (m, 4, $\text{H}_7[\text{A,B}]$); ^{13}C NMR (CDCl_3 , 400 MHz, relative to TMS) -3.9 (Si-CH_3), 18.2 ($\text{CH}_3\text{-C}$), 26.8 (C-CH_3), 130.0 ($\text{C}_3[\text{A}]$), 145.6 ($\text{C}_{3a}[\text{A}]$), 124.0 ($\text{C}_4[\text{A}]$), 123.8 ($\text{C}_5[\text{A}]$), 123.9 ($\text{C}_6[\text{A}]$), 121.9 ($\text{C}_7[\text{A}]$), 137.9 ($\text{C}_{7a}[\text{A}]$), 131.5 ($\text{C}_1[\text{A}]$), 127.0 ($\text{C}_3[\text{B}]$), 136.6 ($\text{C}_{3a}[\text{B}]$), 122.0 ($\text{C}_4[\text{B}]$), 124.9 ($\text{C}_5[\text{B}]$), 125.0 ($\text{C}_6[\text{B}]$), 121.9 ($\text{C}_7[\text{B}]$), 136.7 ($\text{C}_{7a}[\text{B}]$), 126.1 ($\text{C}_1[\text{B}]$).

(b) Crystal Structure Determination of 3,3'-bis(*tert*-butyldimethylsilyl)-1,1'-biisothianaphthene. (1) *Crystal data:* $\text{C}_{28}\text{H}_{38}\text{S}_2\text{Si}_2$, MW = 494.88, triclinic, $a = 7.484(4)$ Å, $b =$

$12.910(4)$ Å, $c = 16.138(5)$ Å, $\alpha = 68.51(2)^\circ$, $\beta = 83.60(3)^\circ$, $\gamma = 87.86(3)^\circ$, $V = 1441.8(9)$ Å³, space group $P\bar{1}$, $Z = 2$, yellow blocks, $0.50 \times 0.50 \times 0.20$ mm³.

(2) *Data collection:* Siemens P4-PC diffractometer, ω -scan mode, graphite-monochromated Mo K α radiation, 5213 reflections measured, 4122 unique reflections (merging $R = 0.0306$ after absorption correction). Three check reflections measured every 100 reflections showed no significant decrease in intensity.

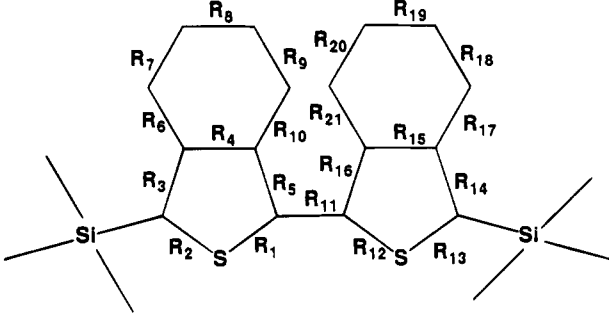
(3) *Structure analysis and refinement:* direct methods, full matrix least-squares on F^2 using SHELXTL-93¹⁹ with all non-hydrogen atoms anisotropic, hydrogen atoms with isotropic U 1.2 times U_{eq} of the parent atom. Final R_1 and $\bar{w}R_2$ values are 0.0393 and 0.0953, respectively, for 3392 $F > 4\sigma(F)$. Siemens SHELXTL-PLUS²⁰ was used for all other calculations and drawings. The list of atomic coordinates has been deposited with the Cambridge Crystallographic Data Centre.

4. Results and Discussion

(a) Geometries. The AM1-optimized geometries of the oligomers are, as expected, typical of an aromatic conjugated backbone; the α - β carbon-carbon bonds of the thiophene subunit are rather short (1.40–1.41 Å) while the β - β carbon-carbon bonds have a single-bond character (*ca.* 1.45 Å). The interring bond length is calculated to be short (1.42 Å) compared to X-ray diffraction measurements performed on thiophene oligomers.^{21–26} This feature has already been reported in previous calculations⁷ and is typical of the AM1 parameterization. The dihedral angle (θ) formed by the planes of two adjacent rings is calculated to be 151.6°, the two sulfur atoms thus pointing in opposite directions (anti conformer). These optimized geometries are similar to those calculated with the AM1 method on unsubstituted aromatic isothianaphthene oligomers.⁷

The experimental geometry of the 3,3'-bis(*tert*-butyldimethylsilyl)-1,1'-biisothianaphthene was obtained by single-crystal X-ray diffraction; the experimental bond lengths for this compound are reported in Table 1 together with the AM1 results. Globally, the AM1-optimized geometry of the dimer is in good agreement with the experimental values. There are, however, some significant differences: (i) The dihedral angle (θ) in the crystal is about 50°, the two sulfur atoms pointing in the same direction. This is in contrast with what is found experimentally in thiophene oligomers, which all adopt an antiplanar conformation in the crystal^{21–26} (note that an anti conformation leads to a reduction of the total dipole moment of the molecule, which is in principle favored). The syn conformation that the molecule adopts in the crystal likely comes as a consequence of packing effects dominated by the bulky side groups, a feature which cannot be taken into account in the calculations. (ii) The calculated bond lengths between carbon and sulfur atoms are shorter by about 0.07–0.08 Å than the experimental data; this feature is related to the AM1 parameterization. (iii) The bond connecting the two isothianaphthene units is measured to be 1.471(4) Å long, which is close to the value determined by X-ray diffraction experiments in thiophene oligomers, ~ 1.45 Å.^{21–26} As expected from the AM1 parameterization, the corresponding calculated value is shorter by about 0.05 Å.

We have therefore carried out a geometry optimization for a dimer where the single interring bond and the dihedral angle (θ) are set at the experimental values, *i.e.*, 1.471 Å and 50°, respectively. The AM1 optimization (see Table 1) shows that the geometry remains clearly aromatic and similar to that calculated for the fully optimized dimer; the main change is the shortening of the R5 distance, but only 0.008 Å, due to the fact that this bond is influenced by the interring bond length.

TABLE 1: Bond Lengths, R_i (Å), of a Disilyl-Terminated Dimer of Isothianaphthalene Obtained at the AM1 Level and by X-ray Diffraction (XRD) Measurements^a


	AM1 ^b	XRD ^c		AM1 ^b	XRD ^c
R_1	1.649	1.721	R_{12}	1.649	1.714
R_2	1.643	1.719	R_{13}	1.643	1.717
R_3	1.401	1.412	R_{14}	1.401	1.415
R_4	1.451	1.446	R_{15}	1.451	1.444
R_5	1.402	1.393	R_{16}	1.402	1.393
R_6	1.424	1.424	R_{17}	1.424	1.431
R_7	1.367	1.364	R_{18}	1.367	1.363
R_8	1.424	1.425	R_{19}	1.424	1.425
R_9	1.368	1.350	R_{20}	1.368	1.356
R_{10}	1.420	1.430	R_{21}	1.420	1.422
R_{11}	1.471	1.471			

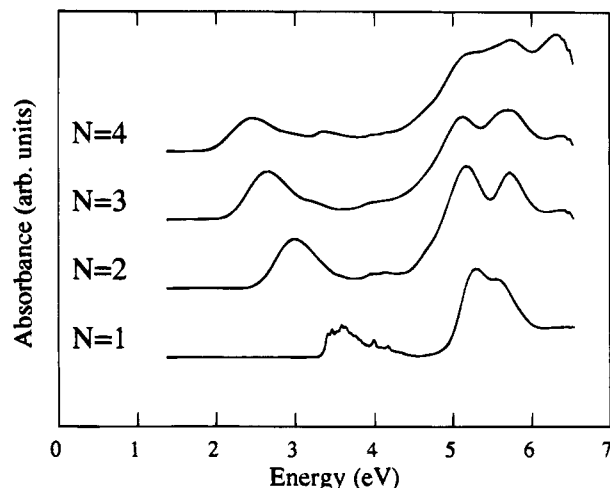
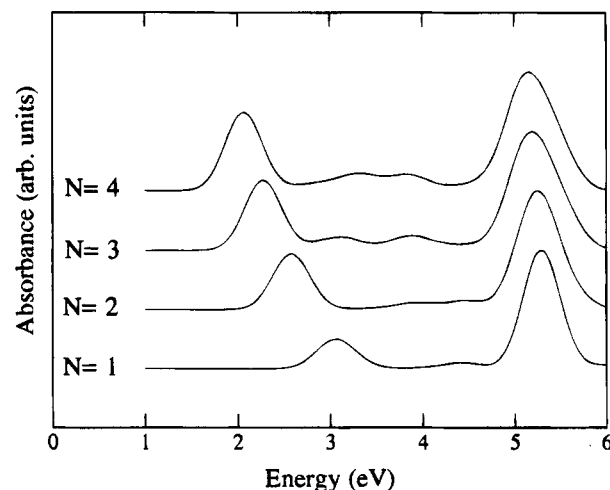
^a The geometry optimization is performed with the interring bond length and the dihedral angle between bonds R_1 – R_{11} – R_{12} forced at 1.471 Å and 50°, respectively. ^b The AM1-optimized geometry possesses a C_2 symmetry. ^c The average standard deviation for the experimental bond lengths (XRD) is 0.004 Å.

Note that we have also considered a system where the two rings are let free to rotate but where the interring bond is fixed to 1.471 Å; in that case, the optimal dihedral angle (θ) is 151.3°, *i.e.*, very close to the value calculated for the dimer without any constraint.

Finally, we have performed geometry optimizations on oligomers (from the dimer up to the tetramer), freezing the interring bond length and the dihedral angle (θ) at 1.471 Å and 130°, respectively. In such a conformation, the systems are out of planarity by 50°, as in the crystal of the dimer, but adjacent sulfur atoms point in opposite directions. This allows us to obtain a linear oligomer chain, instead of the helicoidal conformation induced by a syn conformation between the units. The optimized geometries are calculated to be very close to those of the corresponding syn conformers, the largest bond length difference being on the order of 0.005 Å.

(b) Absorption Spectra. The experimental optical absorption spectra of the oligomers (going from the monomer up to the tetramer) are presented in Figure 2; at least three main peaks or shoulders can be found in the range 2–6 eV. As is expected for conjugated compounds, the first absorption is shifted to lower energies upon increasing the length of the oligomers. The peak positions evolve by 1.12 eV, from 3.58 eV in the monomer down to 2.46 eV in the tetramer. The second transition, which is more intense than the first one, lies at about 5.2–5.3 eV in all spectra, and there occurs a third transition at about 5.8 eV.

In order to rationalize these absorption data, we have simulated at the theoretical level the optical absorption spectra of the four oligomers; at this stage, it must be pointed out that the calculated spectrum of the syn dimer, $\theta = 50.0^\circ$, differs only very slightly from that of the corresponding anti conformer, $\theta = 130.0^\circ$ (small variations appear in the relative intensities of the two peaks, but the transitions occur at the same energies). In solution, it is well-established²² that conjugated chains are more flexible than in the solid state; individual isothianaphthene

**Figure 2.** Experimental optical absorption spectra of the isothianaphthene oligomers recorded in *n*-hexane (N being the number of units).**Figure 3.** Theoretical optical absorption spectra for the 130°-twisted isothianaphthene oligomers (N being the number of units).**TABLE 2: Experimental and Theoretical Positions of the Low-Energy Peak (eV) as a Function of the Number of ITN Units (N)**

N	experimental (<i>n</i> -hexane)	theoretical	
		$\theta = 130^\circ$	$\theta = 180^\circ$
1	3.58	3.03	3.03
2	2.99	2.58	2.40
3	2.65	2.28	1.88
4	2.46	2.07	1.56
6		1.88	1.18

units can thus rotate more easily around the interring bond, solvation energy compensating for the loss of π conjugation. We have therefore considered the conformation with $\theta = 130^\circ$ since it has the advantage of better modeling a linear polymer chain.

The theoretical spectra shown in Figure 3 display two major absorption peaks in the range of energies going from 0 to 6 eV. The first transition is red-shifted as the size of the oligomers (and thus the conjugation length) increases, as observed in the experimental spectra (see Table 2). This absorption is assigned to a $\pi \rightarrow \pi^*$ transition, primarily involving the promotion of one electron from the HOMO to the LUMO; both levels are delocalized (*d*), *i.e.*, the wave functions extend on the whole molecule. For the monomer, the absorption lies at 3.03 eV and goes down to 2.07 eV in the tetramer, *i.e.*, a 0.96 eV shift compared to a 1.12 eV shift in the experimental spectra (Table

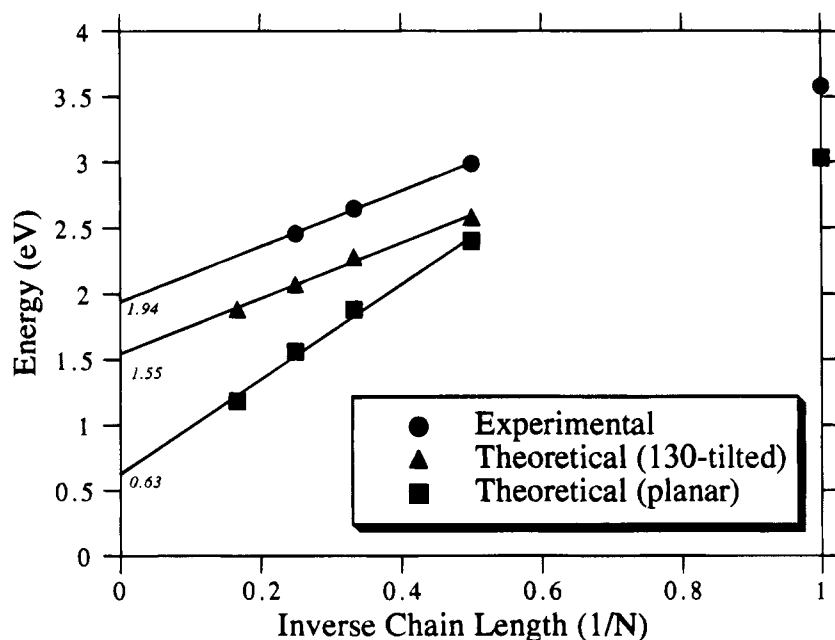


Figure 4. Energy of the HOMO–LUMO transition (eV) vs the inverse of the chain length for the theoretical spectra of the planar and 130°-twisted oligomers and the experimental spectra of the synthesized compounds (N being the number of units).

2). The roughly 0.5 eV difference in peak positions between theory and experiment is not obvious to interpret in detail since many factors can play a role such as the presence of a distribution of conformations in solution, influence of the dielectric medium, geometry differences, or possible shortcomings of the INDO parameterization. The major feature is, however, that the experimental and theoretical results present the same trend, a marked decrease in transition energy as the conjugation length increases. In linear fully aromatic PITN (*i.e.*, in the infinite chain limit), we can thus expect that the first transition occurs at even lower energy, due to extended conjugation; furthermore, in the solid state, packing effects are likely to induce the polymer to adopt a conformation closer to a planar structure, in particular if the end groups are less bulky than those used here for synthetic purposes. This would reduce the band-gap energy even more compared to the transition energies reported in this work for twisted oligomers. Indeed, we calculate that planarity leads to a further decrease of the first transition energy (Table 2); for instance, in the case of the tetramer, the decrease is on the order of 0.5 eV.

Figure 4 represents the evolution of the lowest transition vs the inverse number of units for both the theoretical and experimental spectra. From these data, we extrapolate to the band-gap energy of an infinite chain. As is usually the case when doing such extrapolations, the value for the monomer does not fit linearly with the other data, probably due to the lack of interunit conjugation and it is therefore neglected. At the theoretical level, the linear regression made on four points ($N = 2, 3, 4, 6$) leads to a small energy gap value of 0.63 eV for planar aromatic PITN, which is consistent with our previous VEH results.⁷ Since the torsion of the rings around the interring bond decreases conjugation, the energy difference between the valence band and the conduction band leads to an extrapolated value of 1.55 eV for the 130°-twisted polymer. The band-gap energy of the polymer, as extrapolated from three experimental points ($N = 2 \rightarrow N = 4$), is estimated to occur at 1.94 eV. Note the similarity in slopes for the theoretical curve of the 130°-twisted chains and the experimental curve; the slope of the theoretical curve for the planar chains is larger, which is again an indication of stronger conjugation. We can thus point out that (i) the molecules adopt a strongly nonplanar conformation

in solution because the chains are highly flexible, *i.e.*, the isothianaphthene units can easily undergo rotations around the interring bond, which will drastically reduce the π conjugation in the polymer, and (ii) aromatic planar PITN should possess an energy gap value much lower than that estimated from the spectra recorded in this work.

It is also important to mention that calculations performed on analogous oligomers in the quinoid form indicate that the first absorption peak lies at higher energies than in the corresponding planar aromatic molecules (*e.g.*, 3.11 vs 1.56 eV in the tetramer). Again, this result is consistent with the VEH calculations⁷ and confirms that the planar aromatic form of PITN possesses a lower band-gap energy than the quinoid polymer.

The second absorption peak is calculated to appear around 5.2 eV, in agreement with the experimental spectra. In contrast to the first transition, this peak is only slightly affected by chain length; it varies from 5.29 eV for $N = 1$ to 5.16 eV for $N = 4$. This perfectly matches the evolution observed in the experimental curves; the corresponding peak or shoulder slightly shifts to lower energies, going from 5.30 eV ($N = 1$) to 5.16 eV ($N = 4$). In order to determine the origin of the second peak, we have analyzed the theoretical spectrum of the monomer. In that energy range, the expansion coefficients are significant for three configurations: (i) the first one corresponds to a transition from the HOMO–1 level to the LUMO level; (ii) the second one comes from a HOMO–2 to LUMO transition; and (iii) the last configuration involves the HOMO and LUMO+3 levels; the corresponding orbital wave functions are depicted in Figure 5. The analysis of the LCAO coefficients shows that the orbital wave functions of the occupied levels for the first two configurations (*i.e.*, HOMO–2 and HOMO–1) are mainly localized (1) within the fused phenyl ring. The bonding–antibonding patterns correspond to those of the degenerate HOMO levels in benzene, where the first transition occurs around 6 eV. Globally, the second absorption peak originates from transitions involving localized (HOMO–2 and HOMO–1) and delocalized (HOMO, LUMO, and LUMO+3) π levels. The first two configurations are $1 \rightarrow d^*$ type transitions, whereas the third one is a $d \rightarrow d^*$ type transition. Because of contributions to the second absorption peak coming also from localized levels, we expect that the effect of chain length on

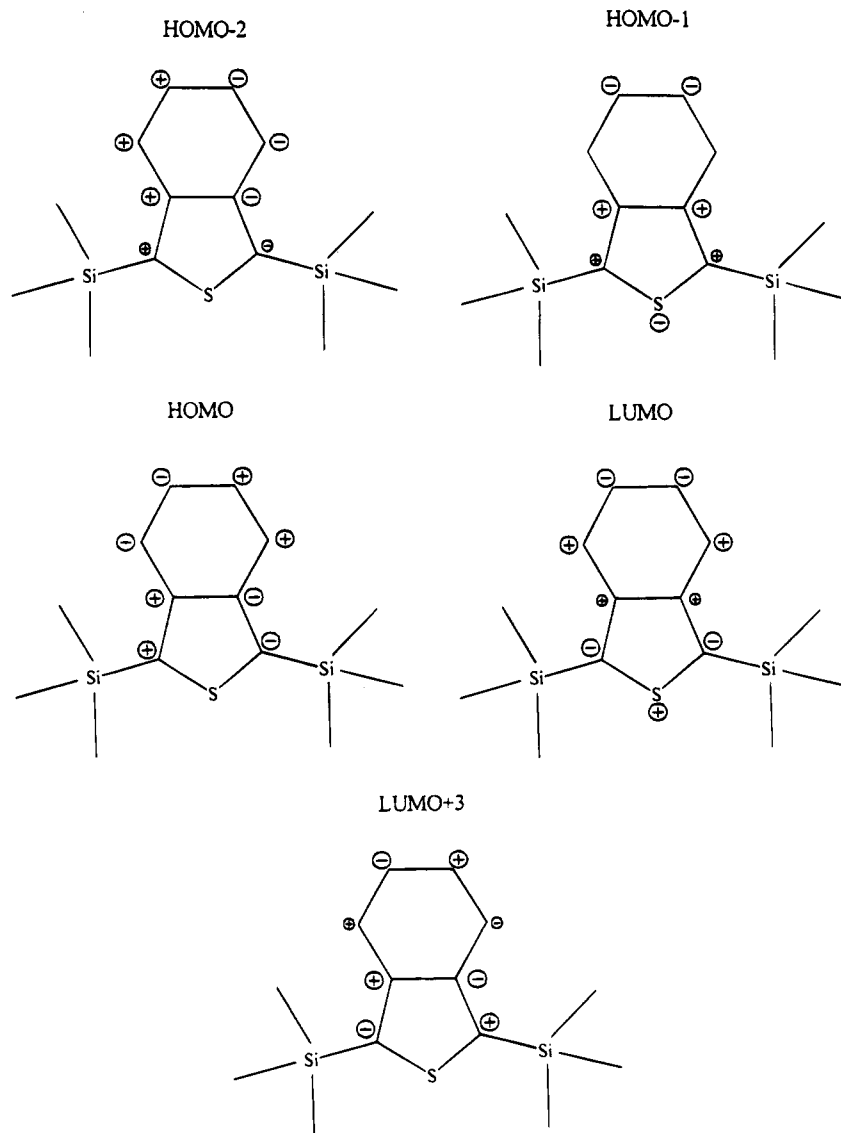


Figure 5. Bonding-antibonding pattern of the molecular orbitals involved in the second absorption peak of the monomer.

the transition energy is weaker than for the first absorption peak which only involves delocalized levels. A similar behavior has been obtained in poly(paraphenylenevinylene) and poly(2,5-dimethoxy-1,4-paraphenylenevinylene) oligomers,²⁷ where the peaks originating from transitions which involve localized levels do not present any significant shift to lower energies as the oligomers become longer.

It is interesting to note that both theoretical and experimental absorption spectra present low-intensity absorption features between the two main peaks. In the case of the monomer, it primarily corresponds to a HOMO to LUMO+4 transition with a weak transition dipole moment.

Finally, we point out that no transition is calculated around 5.8 eV, even though there occurs an absorption that can be observed on all experimental spectra. We believe this discrepancy has to be related to shortcomings in the INDO parameterization with regard to silicon.

5. Synopsis

Using the INDO/SCI formalism, we have analyzed the optical absorption spectra of aromatic isothianaphthene oligomers from the monomer up to the tetramer. Two main absorption peaks are observed in the visible-near UV region. The low-energy absorption, corresponding to a $d \rightarrow d^*$ type transition from the

HOMO level to the LUMO level, is shifted to lower energies when the chain length is increased. The extrapolations made from the HOMO-LUMO transitions of the oligomers to the band-gap energy of aromatic PITN lead to a very small energy gap value of 0.63 eV for the planar system and a value of 1.55 eV for the 130°-twisted infinite chain. The value calculated for the tilted system is in good agreement with the extrapolation of the first energy transition of the oligomers recorded in *n*-hexane, 1.94 eV. These results point out that in solution, the aromatic oligomers adopt a strongly nonplanar conformation, increasing significantly the HOMO-LUMO transition relative to that of a planar aromatic system.

The second strong optical absorption peak is described by electronic excitations involving mostly $l \rightarrow d^*$ transitions. The localized molecular orbitals being less affected by the extent of conjugation than the delocalized levels, the position of the second absorption peak evolves smoothly as the chain length increases, which is in good agreement with the features of the experimental spectra.

Acknowledgment. This work is partly supported by the Belgian Prime Minister Office of Science Policy "Programme d'Impulsion en Technologie de l'Information (IT/SC/22)" and "Pôle d'Attraction Interuniversitaire en Chimie Supramoléculaire et Catalyse", Fonds National de la Recherche Scientifique, and

an IBM Academic Joint Study. One of us (R.K.) is indebted to the Instituut tot aanmoediging van Wetenschappelijk Onderzoek in Nijverheid en Landbouw (IWONL) for a predoctoral fellowship. Financial support from Onderzoeksfonds K. U. Leuven is gratefully acknowledged.

References and Notes

- (1) For recent reviews, see: Proceedings of the International Conference on Science and Technology of Synthetic Metals, Göteborg, August 12–18, 1992. *Synth. Met.* **1993**, 55–57. *Conjugated Polymers*; Brédas, J. L., Silbey, R., Eds.; Kluwer: Dordrecht, 1991.
- (2) Wudl, F.; Kobayashi, M.; Heeger, A. J. *J. Org. Chem.* **1984**, *49*, 3382.
- (3) Lee, Y. S.; Kertesz, M. *J. Chem. Phys.* **1988**, *88*, 2609.
- (4) Nayak, N.; Marynick, D. S. *Macromolecules* **1990**, *23*, 2237.
- (5) Karpfen, A.; Kertesz, J. *J. Phys. Chem.* **1991**, *95*, 7680.
- (6) Kürti, J.; Surján, P. R. *J. Chem. Phys.* **1990**, *92*, 3247.
- (7) Hoogmartens, I.; Adriaensens, P.; Vanderzande, D.; Gelan, J.; Quattrocchi, C.; Lazzaroni, R.; Brédas, J. L. *Macromolecules* **1992**, *25*, 7347.
- (8) Hoogmartens, I.; Adriaensens, P.; Carleer, R.; Vanderzande, D.; Martens, H.; Gelan, J. *Synth. Met.* **1992**, *51*, 219.
- (9) Okuda, Y.; Lakshminathan, M. V.; Cava, M. P. *J. Org. Chem.* **1991**, *56*, 6024.
- (10) Brédas, J. L.; Heeger, A. J.; Wudl, F. *J. Chem. Phys.* **1986**, *85*, 4673.
- (11) Brédas, J. L.; Chance, R. R.; Silbey, R.; Nicolas, G.; Durand, P. *J. Chem. Phys.* **1981**, *75*, 255; **1982**, *77*, 371.
- (12) Dewar, M. J. S.; Zoebisch, E. J.; Healy, E. F.; Stewart, J. J. P. *J. Am. Chem. Soc.* **1985**, *107*, 3902.
- (13) Pople, J. A.; Beveridge, D. L.; Dobosh, P. A. *J. Chem. Phys.* **1967**, *47*, 2026.
- (14) Zerner, M. C.; Loew, G. H.; Kichner, R. F.; Mueller-Westerhoff, J. *J. Am. Chem. Soc.* **1980**, *102*, 589.
- (15) Ridley, J.; Zerner, M. *Theor. Chim. Acta (Berlin)* **1973**, *32*, 111.
- (16) Mataga, N.; Nishimoto, Z. *Phys. Chem.* **1957**, *13*, 140.
- (17) Reissert, A.; Holle, H. *Chem. Ber.* **1911**, 3027.
- (18) Kiebooms, R.; Hoogmartens, I.; Adriaensens, P.; Vanderzande, D.; Gelan, J. *Synth. Met.* **1992**, *52*, 395.
- (19) Sheldrick, G. M. *SHELXL-93, Program for crystal structure refinement*; University of Göttingen: Göttingen, Germany, 1993.
- (20) *SHELXTL*, 1990. *PC Manual*, Version 4.1; Siemens Analytical X-ray Instruments, Inc.: Madison, WI, 1990.
- (21) Hotta, S.; Waragai, K. *J. Mater. Chem.* **1991**, *1*, 835.
- (22) Barbarella, G.; Zambianchi, M.; Bongini, A.; Antolini, L. *Adv. Mater.* **1992**, *4*, 282.
- (23) Barbarella, G.; Zambianchi, M.; Bongini, A.; Antolini, L. *Adv. Mater.* **1993**, *5*, 834.
- (24) Herrema, J. K.; Wildeman, J.; van Bolhuis, F.; Hadziioannou, G. *Synth. Met.* **1993**, *60*, 239.
- (25) Alemán, C.; Brillas, E.; Davies, A. G.; Fajará, L.; Giró, D.; Juliá, L.; Pérez, J. J.; Ruis, J. *J. Org. Chem.* **1993**, *58*, 3091.
- (26) DeWitt, L.; Blanchard, G. J.; LeGoff, E.; Benz, M. E.; Liao, J. H.; Kanatzidis, M. G. *J. Am. Chem. Soc.* **1993**, *115*, 12158.
- (27) Cornil, J.; Beljonne, D.; Friend, R. H.; Brédas, J. L. *Chem. Phys. Lett.* **1994**, *223*, 82.

JP9415119